ACS APPLIED MATERIALS & INTERFACES

Research Article

www.acsami.org

High Yield Growth of Patterned Vertically Aligned Carbon Nanotubes Using Inkjet-Printed Catalyst

James D Beard,*[,†] Jonathan Stringer,[‡] Oana R Ghita,[†] and Patrick J Smith[‡]

[†]College of Engineering, Mathematics and Physical Sciences, University of Exeter, North Park Road, Exeter EX4 4QF, United Kingdom

[‡]Department of Mechanical Engineering, Kroto Research Institute, University of Sheffield, Broad Lane, Sheffield S3 7HQ, United Kingdom

ABSTRACT: This study reports on the fabrication of vertically aligned carbon nanotubes localized at specific sites on a growth substrate by deposition of a nanoparticle suspension using inkjet printing. Carbon nanotubes were grown with high yield as vertically aligned forests to a length of approximately 400 μm. The use of inkjet printing for catalyst fabrication considerably improves the production rate of vertically aligned patterned nanotube forests compared with conventional patterning techniques, for example, electron beam lithography or photolithography.

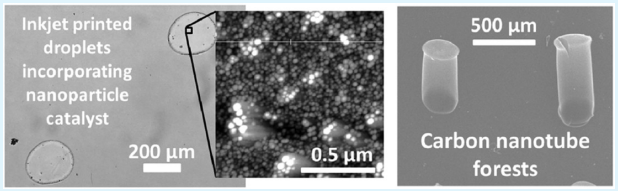

KEYWORDS: *vertically aligned CNT, inkjet printing, patterning, carbon nanotubes, nanoparticles*

INTRODUCTION

Since they were brought to the attention of the scientific world by Iijima,[1] carbon nanotubes have attracted significant research interest as novel electronic devices, sensors, functional coatings and high tensile strength materials. A number of techniques have been applied for their fabrication, including laser- or arc-discharge methods,[2] and chemical vapor deposition (CVD). CVD production of carbon nanotubes can be achieved using a thin-film metal catalyst layer on a growth substrate such as silicon, and hydrocarbon gases as a carbon source.[3,4]

In the CVD process, carbon nanotubes are often observed to grow from the catalyst as vertically aligned carbon nanotube (VA-CNT) "forests", perpendicular to the growth substrate and having strong parallel alignment between nanotubes. Their exceptional electronic and mechanical properties, as well as their very large internal surface area, mean that these vertically aligned nanotube forests are of great interest for applications such as electrodes in supercapacitors,[5] sensing devices,[6] heat dissipation systems,[7] dry adhesives,[8] and reinforcements in composite materials.[9−11] Fabrication of these devices often relies on patterning the catalyst film using standard lithography techniques such as electron beam lithography (EBL) or photolithography, which allow the localization of the nanotubes at particular sites on a growth substrate.

Standard lithography methods can result in excellent localization of the carbon nanotube forests on the substrate; however, standard patterning techniques require multiple processing stages and often require high vacuum environments, increasing processing time and limiting the scalability of the fabrication process. Inkjet printing is a noncontact, additive fabrication process that deposits solutions and suspensions without the need to use masks. In addition to standard graphical applications, inkjet printing has been used to prepare printed electronic devices,[12] scaffolds for tissue engineering,[13] MRI coils[14] and terahertz split ring resonators.[15]

Although inkjet printing has also previously been used to deposit catalyst nanoparticles for the growth of carbon nanotubes by CVD, previous experiments using inkjet-printed nanoparticle[16] or metal salt[17] solutions have not produced vertically aligned nanotubes. In this paper, we demonstrate for the first time the fabrication of strongly vertically aligned, patterned carbon nanotube forests by a combined inkjet-printing/CVD method. As a single-stage, direct-write method, inkjet printing can produce catalyst substrates much more quickly, allowing rapid prototyping or scalable mass production. Previous studies typically produced only tangled nanotube "mats" within the patterned regions, which did not grow significantly perpendicular to the substrate. Other studies used direct printing of nanotube suspension as a deposition method, which also results in nonaligned nanotubes.[18,19] The capacity to produce vertically aligned nanotubes using inkjet printed catalyst greatly expands the range of applications of printed nanotube devices. For example, the high internal surface area of aligned nanotubes makes them ideal as electrodes in supercapacitor devices.[5] Aligned nanotube forests are also highly desirable as reinforcements in polymer composite materials, since parallel fiber alignment increases the strength of these materials and there is potential to obtain a high volume fraction of nanotubes in the polymer matrix.[9−11]

Received: July 21, 2013
Accepted: September 9, 2013
Published: September 9, 2013

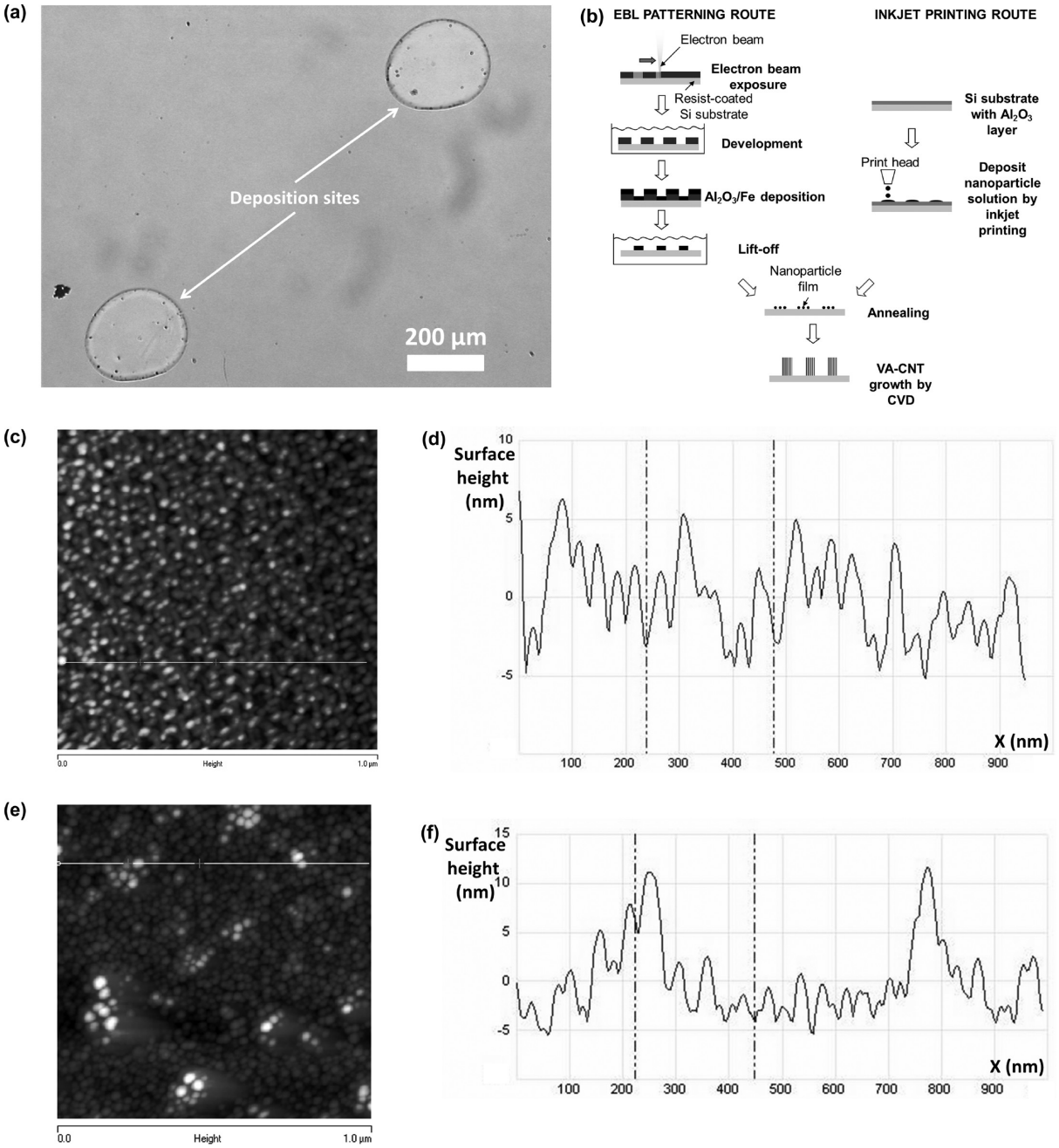

Figure 1. (a) Optical microscope image of drops of catalyst nanoparticles on a substrate after deposition using inkjet printing; (b) flow diagram of electron beam lithography (EBL) and inkjet printing as routes for production of catalyst substrates for growth of VA-CNTs; (c) AFM image of nanoparticles fabricated by annealing of an electron-beam deposited Fe film; (d) profile along white line in (a) showing particle diameter of ~10 nm; (e) AFM image of nanoparticles deposited by inkjet printing of nanoparticle suspension postannealing; (f) profile along white line in (e), showing nanoparticle sizes.

METHOD

Substrates were prepared for inkjet printing by electron beam evaporation of a 45 nm Al_2O_3 film on clean Si wafers with a 100 nm SiO_2 surface layer, as described in our recent paper.[9] The Al_2O_3 film provides an ideal surface for the formation of nanoparticles during the catalyst annealing stage.

A suspension of magnetite nanoparticles in toluene (Fe_3O_4, average particle size 10 nm) of concentration 5 mg/mL was purchased from Sigma-Aldrich (Sigma-Aldrich Company Ltd., Dorset, U.K.) and used as received. Inkjet printing was carried out on a JetLab 4xl printing system (Microfab, Inc., Plano, TX) equipped with a 60 μm diameter drop-on-demand printhead (MJ-AT-01-60, Microfab, Inc.). Ejection of a droplet was achieved by excitation of the printhead with an electrical pulse. The electrical pulse used had an amplitude of 28 V and a duration of 32 μs at a frequency of 1000 Hz. Drops were ejected in a 8 × 8 square array with a spacing between deposition sites of 1 mm. The number of droplets ejected at each deposition site was varied, with either 1, 8, 27, or 64 droplets deposited per deposition site. The accumulation of multiple drops at each site resulted in drop diameters of approximately 144 ± 5, 238 ± 15, 330 ± 10, and 450 ± 30 μm, respectively (measured via optical microsope). An optical image of nanoparticle drops deposited using inkjet printing is shown in Figure 1a.

For comparison with the inkjet printed samples, catalyst patterning was also carried out by EBL using standard lithography methods. A 500 nm PMMA resist film was deposited onto a Si wafer, and

dx.doi.org/10.1021/am402942q | ACS Appl. Mater. Interfaces 2013, 5, 9785−9790

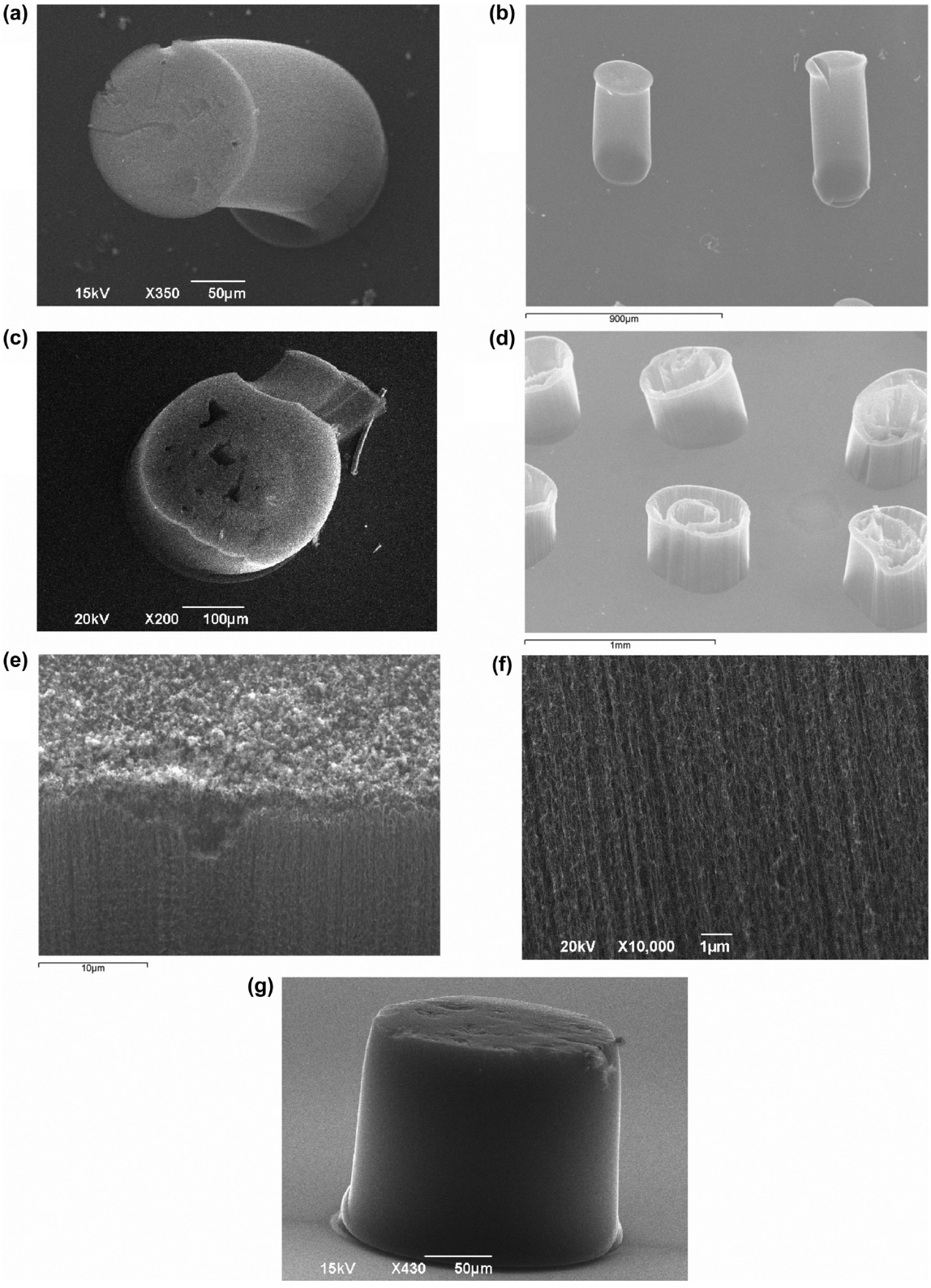

Figure 2. (a–d) SEM images of vertically aligned carbon nanotube forests localized at catalyst sites deposited by inkjet printing, using (a) 1, (b) 8, (c) 27, (d) 64 drops/site. The 27- and 64-drop sites show less uniform growth than those grown with 1 and 8 drops/site, with vacancies within the nanotube forests. The forests in (d) show vertically aligned growth concentrated in concentric rings within the deposition site. These rings may arise due to the "coffee-ring" effect that produces nonuniform distribution of catalyst particles within the printed region. (e) Magnified view of nanotube forest sidewall, from a forest grown using 64 drops/site of catalyst suspension, showing strong vertical alignment within the forest capped by a disordered "tangle" at the forest top. (f) Increased magnification image of forest sidewall, in this case from a forest grown using 27 drops/site, showing CNT alignment. (g) Example of a nanotube forest grown using catalyst patterned by electron beam lithography (EBL) for comparative purposes.

patterned using a scanning electron microscope (SEM) system. The resist was developed using a 15:5:1 IPA/MIBK/EMK (isopropyl alcohol/4-methylpentan-2-one/ethyl methyl ketone) mix and washed with IPA prior to deposition of Al_2O_3/Fe films by electron beam evaporation (of 45 nm/2 nm thickness, respectively) as described in our paper,[9] followed by PMMA removal ("lift-off") with acetone at room temperature and cleaning with IPA prior to CVD.

CVD growth took place in a SabreTube desktop thermal processing system incorporating a suspended silicon platform substrate heater[20] and an external quartz tube preheater,[21] which allowed separate thermal treatment of the precursor gases. This process is described in more detail in a previous paper.[9] The two methods of catalyst production (EBL and inkjet printing) are shown schematically in Figure 1b.

The printed substrates were preannealed in a reducing atmosphere composed of He/H_2 at ~800 °C for 2 min, prior to introduction of ethylene gas to the heated substrate as a carbon source for carbon nanotube growth. The gases were pretreated in the external preheater at 990 °C before introduction to the growth substrate; this causes decomposition of the gases into carbonaceous fractions.

SEM imaging was carried out using a Hitachi S3200N SEM-EDS system, with some images taken using a JEOL JSM-6390LV SEM system. Atomic Force Microscope (AFM) imaging was carried out in tapping mode using a Bruker Innova AFM and Bruker MPP-11123 tapping mode probes, with spring constant and resonant frequency of approximately 40 N/m and 300 kHz, respectively, with a scan rate of 0.5−1 Hz.

RESULTS

AFM imaging was used to examine catalyst particles, both on samples patterned by inkjet printing and by EBL. In the case of the films patterned using EBL, catalyst particles are formed by annealing the electron beam deposited Fe films. Annealing was carried out at ~800 °C for 2 min using the same process as was used prior to nanotube growth, omitting the introduction of ethylene gas so that no nanotubes were produced. AFM images of the annealed electron beam deposited Fe films showed the presence of approximately 10 nm diameter nanoparticles on the substrate surface. An example image is shown in Figure 1c,d.

Annealing was also carried out on the inkjet-printed samples under the same conditions. AFM imaging of these samples was carried out both pre- and postannealing; preannealing, the inkjet printed samples showed significant contamination, probably from the solvent and surfactants used to disperse the nanoparticles, which prevented the acquisition of good images by AFM. AFM imaging of the annealed inkjet printed samples, however, showed similar particles to those of the annealed electron beam deposited films, as shown in Figure 1e, and did not show any signs of contamination. This suggests that the inkjet printed Fe_3O_4 suspension forms a nanoparticle film upon annealing similar to that produced from the annealed electron beam deposited films. This also suggests that the annealing process removes the majority of the solvent contamination by evaporation or chemical breakdown. The size of the nanoparticles (~10 nm) can be determined from the profile shown in Figure 1f; the lateral size of the particles shown in Figure 1e appears larger than 10 nm due "sample broadening" caused by convolution with the probe tip size, which occurs during AFM imaging.[22] The similar size of the Fe_3O_4 nanoparticles on the substrate compared to the supplied nanoparticle size also shows that little particle growth occurs due to the annealing process and that the size of the catalyst particles is therefore controlled by the size of deposited Fe_3O_4 nanoparticles.

Chemical vapor deposition using ethylene gas as a precursor was used to produce carbon nanotube forests from the inkjet printed and EBL-patterned catalyst substrates. The forest height was monitored *in situ* during growth using a laser interferometer, with the nanotubes grown on inkjet-printed substrates attaining a height of 0.4 mm. SEM images of these nanotube forests are shown in Figure 2a−f. The SEM images showed localization of the carbon nanotube growth within the regions of printed catalyst, with strong parallel alignment of the nanotubes perpendicular to the growth substrate capped by a disordered "tangle" region at the forest crown. Nanotube forests grown using inkjet printed catalyst appeared very similar to those produced using EBL-patterned substrates under the same growth conditions, an example of which is shown in Figure 2g. This illustrates that the inkjet-printing technique is comparable to the more widely used lithographic patterning methods for the deposition of catalysts for the growth of vertically aligned carbon nanotube forests.

The SEM images suggested that a highly uniform growth of VA-CNTs was obtained on regions printed using 1−8 drops/site, as shown in Figure 2a,b. In larger printed regions (27 and 64 drops/site), nanotube growth was not as uniform. The nanotube forests still exhibit strong vertical alignment; however, many of these forests contained "vacancies" where vertically aligned growth was not visible, as shown in Figure 2c,d. For the largest printed regions (64 drops/site), vertically aligned nanotube growth was concentrated in concentric rings, including at the boundary of the printed region. Examples of this effect can be seen in Figure 2d. This may be attributed to the `coffee-ring" effect often observed in the distribution of nanoparticles deposited by inkjet printing, where the solvent evaporation process concentrates the particles at the edges of the drop.[23,24] This would concentrate the catalyst particles in ring-like regions on the substrate and, therefore, result in a ring-shaped distribution of carbon nanotube growth. The presence of multiple rings may arise due to a "stick−slip" motion of the edge of the drop during drying, creating radial variation in nanoparticle density.

DISCUSSION

Alignment of CVD-fabricated nanotubes occurs when the growing nanotubes reach a critical surface density on the growth substrate; after this point, there is not enough space for lateral growth and the nanotubes can only continue to grow perpendicular to the substrate. Parallel alignment is maintained by the high nanotube stiffness and strong intertube van der Waals attraction.[25] The presence of vertical alignment in these samples indicates that we are able to achieve a high yield of carbon nanotubes. This high yield is attributable to two factors. First, the CVD process used, incorporating thermal pretreatment of the reactant gas separate from the heated catalyst substrate, is known to produce high nanotube yields resulting in the production of vertically aligned nanotubes.[21,26] This is attributed to the decoupling of the gas treatment and substrate annealing temperatures, allowing these temperatures to be optimized independently to attain tall nanotube forests. Second, successful growth of carbon nanotube forests using thin-film or nanoparticle catalysts is dependent on the distribution of catalyst nanoparticles formed during the inkjet printing and initial catalyst annealing process. A particle monolayer has been found to be ideal for aligned nanotube growth; the close packing of particles produces a high nanotube density, leading to self-alignment of the nanotubes.[27] Under the

assumption that there is minimal segregation of particles upon evaporation of the droplet, a simple model for the propensity of monolayer formation can be constructed. The volume of nanoparticles that are deposited in each sample (V_p) is as follows (eq 1):

$$V_p = V_0 n f \tag{1}$$

Where V_0 is the volume of a single droplet, n is the number of droplets deposited, and f is the volume fraction of nanoparticles within the ink. For a monolayer to form, there must be sufficient nanoparticles to cover the contact area between deposited ink and substrate. The formed monolayer will therefore have a volume equal to a prism of cross section equal to the contact area (A) and length equal to the diameter of a nanoparticle (h). The volume of nanoparticles required to form such a monolayer will be equal to the volume of the prism multiplied by the packing efficiency of the particles (ξ). This leads to the following (eq 2):

$$V_p = Ah\xi \tag{2}$$

Assuming that the nanoparticles are spherical enables the value of ξ to be estimated by calculating the packing efficiency of a single layer of close packed spherical particles, whereupon it is found that[28] $\xi = \pi/3\sqrt{3}$.

Because of an inkjet printed droplet having a Bond number ($Bo = \rho g D_0^2/\sigma$, where ρ is density of the ink, g is acceleration due to gravity, and σ is the ink surface tension) significantly below 1, the contact area of the droplet with the substrate is controlled by the balance of surface energy between the ink, substrate and surroundings.[29] On a homogeneous, flat, substrate, it would therefore be expected that a droplet would spread to form a spherical cap, with the contact diameter dependent upon the contact angle between the ink and the substrate.[29] For a deposited volume of liquid made up of multiple droplets, if evaporation is assumed to be negligible between droplet depositions, a droplet diameter equivalent to a single spherical droplet of volume equal to the multiple droplets, D_1, can be calculated:

$$\frac{\pi D_1^3}{6} = \frac{\pi D_0^3}{6} n \tag{3}$$

Using this relationship, and the ratio between the spread diameter and initial droplet diameter as a function of contact angle,[29] β, an expression for the contact area as a function of β, D_0 and n can be derived:

$$A = \frac{\pi \beta^2 D_0^2 n^{2/3}}{4} \tag{4}$$

By substituting eq 4 into eq 2, an expression for the volume of a formed monolayer is obtained. This can then be equated with eq 1 to obtain:

$$\frac{1}{6} D_0 n^{1/3} f = \frac{1}{4} \beta^2 h \xi \tag{5}$$

In eq 5, the only variable that is not determined by the ink/substrate combination used within the work is n. The requisite number of printed droplets to achieve a monolayer can therefore be calculated with the following:

$$n = \left(\frac{3\beta^2 \xi h}{2 D_0 f} \right)^3 \tag{6}$$

If the number of droplets is less than that calculated using eq 6, an incomplete monolayer would be expected to form, whereas a greater value of n would result in too many particles being present, inhibiting the formation of a particle monolayer during the catalyst annealing phase and the subsequent growth of vertically aligned nanotubes.

Under the conditions used in this work, appropriate values are D_0 = 60 μm (printhead nozzle diameter), β = 2.37 (calculated from images of single deposited droplet), h = 14 nm (average magnetite nanoparticle diameter, with the addition of the length of 2 oleic acid molecules, the surfactant used to stabilize the magnetite dispersion[30]). The volume fraction, f, was calculated to be 0.000966 by dividing the nanoparticle concentration of 5 mg/mL by the density of Fe_3O_4 (5170 kg/m^3). Using these values gives an optimal number of droplets per sample of 1.84. The optimal number of droplets predicted by the model is likely to be an underestimate due to presence of coffee staining, as a proportion of the deposited nanoparticles would segregate to the periphery of the droplet. Taking this into account, it is most likely that the optimum number of droplets will be greater than 1.84, although this has yet to be quantified. Both samples with a number of drops closest to the optimum (1 drop and 8 drop) were most successful in producing a high yield of nanotubes, with higher numbers of drops (27 drop and 64 drop) producing significantly lower yields. This is in good qualitative, and reasonable quantitative, agreement with the model.

CONCLUSION

In summary, we have demonstrated the successful growth of patterned vertically aligned carbon nanotube forests using inkjet printed nanoparticle catalyst, attaining nanotube forests similar to those produced under the same CVD conditions using catalyst patterned by electron beam lithography. This rapid, single-stage method of catalyst fabrication by a direct-write method has significant advantages over standard multi-stage lithography methods such as EBL and photolithography, due to its much lower processing time.

The strong vertical alignment displayed by these forests has been attributed to a high yield of nanotubes. This is likely due to good distribution of catalyst nanoparticles on the substrate surface combined with two-stage thermal treatment of the CVD reactant gases and catalyst, decoupling the gas treatment temperature from the substrate annealing process.

On the basis of these experiments, a model has been proposed for the optimum concentration of nanoparticles required to form a monolayer of catalyst particles within the deposited regions ideal for the growth of vertically aligned carbon nanotubes. The high yield of nanotubes from samples which, according to our model, should have a greater surface density of nanoparticles than that necessary to form a monolayer shows that aligned nanotube growth is also possible from denser particle distributions. The ideal distribution of inkjet printed catalyst on substrates could therefore form the subject of future studies.

This paper is the first to report on growth of high yield VA-CNT using nanoparticle catalyst patterned by inkjet printing. However, as discussed above, there are areas which need to be explored in further detail to control and optimize this process. In future, this method could be used for rapid production of patterned, vertically aligned carbon nanotube forests for a wide range of applications. The inkjet-printing method is highly scalable and could be suited to rapid prototyping or to mass

production of devices. Inkjet printing also has the potential advantage of better control of the size and distribution of the nanoparticles, which could allow improvement and optimization of the nanotube forest density for different applications.

AUTHOR INFORMATION

Corresponding Author

*James D. Beard, Room 221, Harrison Building, North Park Road, Streatham Campus, University of Exeter, Exeter EX4 4QF UK. Telephone: 01392 263 617. E-mail: jb523@ex.ac.uk.

Notes

The authors declare no competing financial interest.

ACKNOWLEDGMENTS

The manuscript was written through contributions of all authors. All authors have given approval to the final version of the manuscript. The authors would like to acknowledge EADS Innovation Works for providing funding for this research, and would also like to thank Dr. Lesley Wears of the University of Exeter for her assistance in our electron microscopy imaging.

REFERENCES

(1) Iijima, S. *Nature* **1991**, *354*, 56−58.
(2) Bethune, D. S.; Klang, C. H.; De Vries, M. S.; Gorman, G.; Savoy, R.; Vazquez, J.; Beyers, R. *Nature* **1993**, *363*, 605−607.
(3) Jose-Yacaman, M.; Miki-Yoshida, M.; Rendon, L.; Santiesteban, J. G. *Appl. Phys. Lett.* **1993**, *62*, 202−204.
(4) Hart, A. J.; Slocum, A. H. *J. Phys. Chem. B* **2006**, *110*, 8250−8257.
(5) Kim, B.; Chung, H.; Kim, W. *Nanotechnology* **2012**, *23*, 155401.
(6) Wang, Y.; Yeow, J. T. W. *J. Sens.* **2009**, *2009*, 493904.
(7) Huang, H.; Liu, C. H.; Wu, Y.; Fan, S. *Adv. Mater.* **2005**, *17*, 1652−1656.
(8) Qu, L.; Dai, L.; Stone, M.; Xia, Z.; Wang, Z. L. *Science* **2008**, *322*, 238−242.
(9) Allen, R. J.; Ghita, O.; Farmer, B.; Beard, M.; Evans, K. E. *Compos. Sci. Technol.* **2013**, *77*, 1−7.
(10) Garcia, E. J.; Hart, A. J.; Wardle, B. L.; Slocum, A. H. *Adv. Mater.* **2007**, *19*, 2151−2156.
(11) Li, X.; Gao, H.; Scrivens, W. A.; Fei, D.; Xu, X.; Sutton, M. A.; Reynolds, A. P.; Myrick, M. L. *Nanotechnology* **2004**, *15*, 1416.
(12) Perelaer, J.; Smith, P. J.; Mager, D.; Soltman, D.; Volkman, S. K.; Subramanian, V.; Korvink, J. G.; Schubert, U. S. *J. Mater. Chem.* **2010**, *20*, 8446−8453.
(13) Zhang, Y.; Tse, C.; Rouholamin, D.; Smith, P. J. *Cent. Eur. J. Eng.* **2012**, *2*, 325−335.
(14) Mager, D.; Peter, A.; Del Tin, L.; Fischer, E.; Smith, P. J.; Hennig, J.; Korvink, J. G. *IEEE Trans.. Med. Imaging* **2010**, *29*, 482−487.
(15) Walther, M.; Ortner, A.; Smith, P. J.; Meier, H.; Loffelmann, U.; Korvink, J. G *Appl. Phys. Lett.* **2009**, *95*, 251107−251107−3.
(16) Ago, H.; Qi, J.; Tsukagoshi, K.; Murata, K.; Ohshima, S.; Aoyagi, Y.; Motoo Yumura, M. *J. Electroanal. Chem.* **2003**, *559*, 25−30.
(17) Chatzikomis, C.; Pattinson, S. W.; Koziol, K. K. K. K.; Hutchings, I. M. *J. Mater. Sci.* **2012**, *47*, 5760−5765.
(18) Chen, P.; Fu, Y.; Aminirad, R.; Wang, C.; Zhang, J.; Wang, K.; Galatsis, K.; Zhou, C. *Nano Lett.* **2011**, *11*, 5301−5308.
(19) Kordas, K.; Mustonen, T.; Toth, G.; Jantunen, H.; Lajunen, M.; Soldano, C.; Talapatra, S.; Kar, S.; Vajtai, R.; Ajayan, P. M. *Small* **2006**, *2*, 1021−1025.
(20) van Laake, L.; Anastasios John Hart, A. J.; Slocum, A. H. *Rev. Sci. Instrum.* **2007**, *78*, 083901.
(21) Meshot, E. R.; Plata, D. L.; Tawfick, S.; Zhang, Y.; Verploegen, E. A.; Hart, A. J. *ACS Nano* **2009**, *3*, 2477−2486.
(22) Markiewicz, P.; Goh, M. C. *J. Vac. Sci. Technol., B* **1995**, *13*, 1115−8.
(23) Tekin, E.; Smith, P. J.; Schubert., U. S. *Soft Matter* **2008**, *4*, 1072−1078.
(24) Deegan, R. D.; Bakajin, O.; Dupont, T. F.; Huber, G.; Nagel, S. R.; Witten, T. A. *Phys. Rev. E* **2000**, *62*, 756−765.
(25) Fan, S.; Chapline, M. G.; Franklin, N. R.; Tombler, T. W.; Cassell, A. M.; Dai, H. *Science* **1999**, *283*, 512−514.
(26) de Villoria, R. G.; Hart, A. J.; Wardle, B. L. *ACS Nano* **2011**, *6*, 4850−4857.
(27) Zhang, G.; Mann, D.; Zhang, Li.; Javey, A.; Yiming, Li.; Yenilmez, E.; Wang, Qian.; McVittie, J. P.; Nishi, Y.; Gibbons, J.; Dai, H. *Proc. Natl. Acad. Sci. U.S.A.* **2005**, *102*, 16141−16145.
(28) Dushkin, C. D.; Lazarov, G. S.; Kotsev, S. N.; Yoshimura, H.; Nagayama, K. *Colloid Polym. Sci.* **1999**, *277*, 914−930.
(29) Stringer, J.; Derby, B. *J. Eur. Ceram. Soc.* **2009**, *29*, 913−918.
(30) Zhang, L.; He, R.; Gu, H.-C. *Appl. Surf. Sci.* **2006**, *253*, 2611−2617.